Shaik et al., *Cogent Engineering* (2019), 6: 1616373
https://doi.org/10.1080/23311916.2019.1616373

cogent engineering

PRODUCTION & MANUFACTURING | RESEARCH ARTICLE

Investigations and optimization of friction stir welding process to improve microstructures of aluminum alloys

Bazani Shaik[1]*, G. Harinath Gowd[2] and B. Durga Prasad[3]

Received: 28 December 2018
Accepted: 5 May 2019
First Published: 10 May 2019

*Corresponding author: Bazani Shaik, Department of Mechanical Engineering, JNTUA, Ananthapuramu, A.P 515002, India
E-mail: bazanimits@gmail.com

Reviewing editor:
Yuegang Yuegang Tan, School of Mechanical and Electronic Engineering, Wuhan University of Technology, Wuhan, China

Additional information is available at the end of the article

Abstract: This work mainly focus on finding the optimal conditions for improving the efficiency of the dissimilar welded joints that were prepared using the friction stir welding (FSW) process. To carry out further research on the FSW process, it is very important to know the significant process parameters. As per the literature, rotational speed, welding speed, and tilt angle are the most significant parameters and hence have been considered in the current investigation on output responses are tensile strength, impact strength, and elongation are the multi-responses identified; they were also investigated with the help of two-dimensional (2D) plots. The experimental design is planned as per the Taguchi L9 orthogonal array. The straight cylindrical threaded tool is used in this work. AL6082-T651 and AL7075-T651 alloys are taken as the workpiece material based on its applications. The workpieces are cut as per the American Society for Testing and Materials standards. After performing the experiments, each output response is measured at all the welding conditions and is tabulated. This experimental data is used for optimizing the multi-responses using the Taguchi Grey relational analysis (GRA) method. This GRA method helps optimize the multi-responses in an FSW process. In the process of optimization using the GRA method, the signal-to-noise ratios, the Grey relational coefficients, and the Grey relational grades are calculated, and ranking will be given based on the Grey relational grade values. Overall, this method proves suitable for optimizing the multi-responses in the FSW process.

Bazani Shaik

ABOUT THE AUTHOR

Bazani Shaik is a Research Scholar at the Mechanical Engineering, JNTUA, Ananthapuramu. He received his Bachelor's degree and Masters Degree in Mechanical Engineering from JNTU in 2009 and 2012, respectively. His Ph.D. research project was in parametric optimization of FSW process to improve microstructures of aluminum alloys, under the supervision of Professor Dr. G. Harinath Gowd from Madanapalle Institute of Technology and Science and Prof. B. Durga Prasad from Jawaharlal Nehru Technological University, the co-authors of this manuscript. Professor Dr. G. Harinath Gowd leads the Production Technology, an industrial engineering research group in the Department of Mechanical Engineering MITS, Angallu and Prof. B. Durga Prasad is a leading researcher in Department of Mechanical Engineering, JNTUACE, Ananthapuramu.

PUBLIC INTEREST STATEMENT

Among all the conventional methods, the recently evolved friction stir welding (FSW) process has become very popular as it is used for welding numerous materials and hard metals, including aluminum, magnesium, and polyethylene, where accuracy is not of prime importance. The objective of this research work involving the FSW process is to conduct an experimental investigation on the process parameters and to study the types of responses. It is hoped that this production process would find wide applications in shipbuilding, aerospace industries, marine, and construction industries.

Subjects: Manufacturing Engineering; Materials Science; Production Engineering

Keywords: Dissimilar welded joints; friction stir welding; Grey relational analysis; Grey relational grade; multi-responses; optimization

1. Introduction

FSW is a revolutionary concept used by industrialists and welding experts because it provides the best solution to address difficulties in automotive and aerospace industries and various applications are used for joining aluminum alloys at high temperature and new opportunities for a relook of the best use of most available metal on earth. Aluminum alloys have various advantages: good corrosion resistance, high formability, high strength, low density, and low weight (Rajesh, Srimuthunath, Santa Kumar, Sugandipriya, & Aravindan, 2018). Mechanical properties and microstructures for the development on dissimilar aluminum alloys 7075Al and 7050Al alloys of tensile strength improves 2195Al,2014Al,2219Al alloys temperature of 175°C and microstructural studies shows the zig-zag line, kissing bond, onion structure and factors of hardness has superplastic behavior of aluminum alloys and controlled fatigue behavior increases welding speed and rotational rate is independent. The weld direction and cross section of weld seam on tilt angle, shoulder, and tool pin are given in Figure 1.

Joining of brass plates (Sundqvist et al., 2017) with 6 mm thickness has been investigated at rotational speeds of 450 and 710 rpm. The higher rotational speeds observed on welding zone defect-free weld zone at rotational speeds is lower due to the formation of cracks and microstructural investigations determined heat affect zone, thermomechanically affected zone, grain size, stir zone has recrystallized zones fine for higher hardness. Dissimilar welds have been studied (Santos, Torres, & Ramirez, 2017) for stainless steel SS AISI 304L and-6Al-4V titanium alloy of butt joint and limitation is tool wear reduced on preheating of the laser beam and developed a mathematical model for calculating tool forces of heat generation of process on the complex reaction of FSW and laser beam. Han, Wan, Yabuuchi, Serizawa, & Kimura, 2018 have investigated joints of 6 mm thick of UNS S 32,101 and S32205 duplex and S32750 and S32760 super duplex stainless steel of tensile strength improved and increased of yield strength and characterization of microstructural refinement grain of welded joint of grain sizes of 1 µm and rotational speed 200 rpm and welding speed 10 0mm/min and axial force 36 kN and possible tool polycrystalline beta nitride with 40%W temperature is maximum at 850°C mechanisms on dynamic recrystallization ductility decrease with the presence of secondary phases is harmful have investigated (Dourandish, Mousavizade, Ezatpour, & Ebrahimi, 2017) joining of martensitic steel and ferritic steel of characterization of inhomogeneity and ferritic steel has a grain size of 2.5 µm and coarser size of 60 µm in base metal and hardening of post weld heat treatment temperature at 750°C for 1 h. Investigated Al2024 (Wahid, Khan, Siddique, Shandley, & Sharma, 2018) of friction stir spot welding by a novel method and increasing of length joint and nugget zone of rotational speed 1,600 rpm, height protrusion 0.4 mm and metallurgic

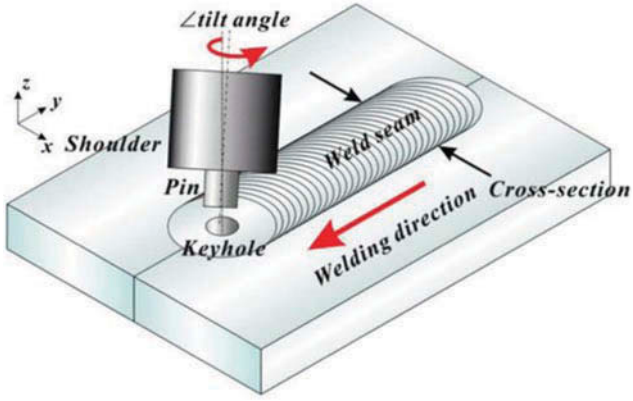

Figure 1. Schematic view of friction stir welding process.

bonding is superior and fine grain size is 0.5 µm due to plastic deformation and dynamic recrystallization nugget zone is more significant compared to joint length. Padhy, Wu, & Gao, (2018) have investigated AL6082-T6 FSW underwater to overcome the problem of peak temperature of-of tensile strength is 241 MPa and base metal strength is 79% and 10.7% conventional air of rotational speed 900 rpm, weld speed 80 mm/min and tool shoulder 17 mm of 10% tensile strength is increased and smaller size of stir zone due to heat intension on plastic deformation observations of grain coarsening on heat affected zone and thermomechanical affected zone of normal fracture due to free joint. Liu et al. (2018a) the emerged friction stir-based welding of review and compile of materials joining of aspects on parameters, features of products on metallurgical feasibility of lesser emerging technologies (Giraud, Robe, Claudin, ChristopheDesrayaud, & Bocher, 2016) have investigated clam steel and 316L stainless steel of different mechanical properties and microstructural investigations studied on the minimum temperature of 620° C. Weld metal is the higher temperature of transformation on heat affected zone of clam is gradually decreased with the increase of post weld heat temperatures optimizes the hardness and excellent on heat affected zone and weld metals of 316L and clam steel. Experimental analyses on dissimilar Al alloys 7020-T651 and 6060T6 showed that they have advanced speeds in the range of 300–1,100 mm/min and rotational speeds in the range of 1,000–2,000 rpm. This article investigates the macro- and microstructural characterization flow in a nugget zone and the mechanical behavior of quasi-static tensile tests and crosses weld microhardness is studied and microstructural computed maps have weak zones.

2. Experimental work

The experiments were carried out using dissimilar Al7075T651 and Al6082T651 (artificially aged due to stretching of stress-relieved and heat-treated solution) aluminum alloys of 6 mm thickness of a straight cylindrical threaded tool shown in Figure 2. Using an M2Grade SHSS tool of shoulder diameter 18 mm and probe length 6 mm on a computer-controlled numerical FSW process. The special-purpose machine was at Annamalai University. The components and arrangement of the plates of FSW are shown in Figure 3. The chemical compositions of material measured alloying elements by the American Society of Metals are shown in Table 1. The plates were finished to a dimension of

Figure 2. Straight cylindrical threaded tool.

Figure 3. Dissimilar weld position of friction stir welding.

Table 1. Chemical compositions of Al7075-T651 and Al6082-T651 (percentage of weight)

Al alloy	Si	Fe	Cu	Mn	Mg	Cr	Ni	Zn	Ti	Al
7075-T651	0.12	0.2	1.4	0.63	2.53	0.2	0.004	5.62	0.03	balance
6082-T651	1.05	0.26	0.04	0.68	0.8	0.1	0.005	0.02	0.01	balance

100 mm × 50 mm×6 mm plates on individually flattering the surfaces of effect for adjusting a mechanism of two pairing edges. A butt weld was made by clamping the materials using fixtures by placing AA7075T651 and AA6082T651 on the advancing side and the retreating side, respectively, by opting the parameters rotational speed (RS), welding speed (WS), and tilt angle (TA) that are investigated for pilot study and literature review, i.e. three levels are shown in Table 2 The test specimens are prepared according to the ASTM standards. Grey relational analysis (GRA) of Taguchi is used on an orthogonal array of L9 selection for responses tensile strength, elongation, impact strength are most important moderation quality of butt joint weld. GRA is used for output variables to get maximum values. The orthogonal array L9 experimental plan is given in Table 3. Al7075T651 in advancing side and Al6082T651 in retreating side are considered the best for joining and development of mechanical properties. The FSW specimens are cut in sections of transverse as per ASTME8. The specimens of tensile tests are shown in Figure 4 and specimens of the impact test are shown in Figure 5. The tensile specimens were tested at room temperature on 100 kN Universal Testing Machine Model F-100. Tensile strength and impact strength test results are shown in Table 4. Elongation percentage is also shown in Table 4. The weld specimens are appropriately prepared for the metallurgical examination and investigated to improve the microstructures of aluminum alloys. The dissimilar welds of Al7075T651 and Al6082T651 were toned with HydroFluoric solution with a magnification of 100×. The microstructural investigations and observation of the material mixing were carried out using an optical microscope.

3. Taguchi-based GRA

The unknown information of a process to determine a system for statistical optimization techniques. The Taguchi method is a powerful technique for optimization of different engineering problems. Characteristics of quality can optimize problem by the Taguchi technique. The

Table 2. Levels of process parameters

Sno	Parameters	Notation	Unit	Levels		
				−1	0	1
1	Rotational speed	RS	rpm	1,150	1,250	1,350
2	Weld speed	WS	mm/min	40	50	60
3	Tilt angle	TA	Degree	1	2	3

Table 3. Experimental plan through the L9 orthogonal array

Exp.no.	Rotational speed (rpm)	Weld speed (mm/min)	Tilt angle (°)
1	−1	−1	−1
2	−1	0	0
3	−1	1	1
4	0	−1	0
5	0	0	1
6	0	1	−1
7	1	−1	1
8	1	0	−1
9	1	1	0

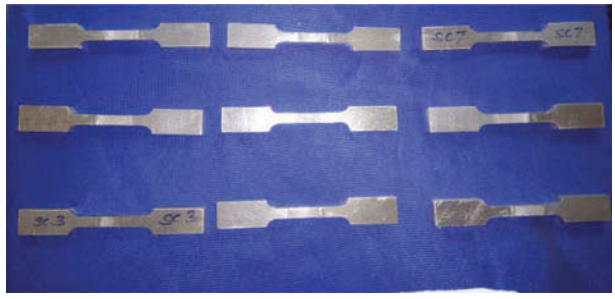

Figure 4. Specimens of the tensile test as per ASTME8.

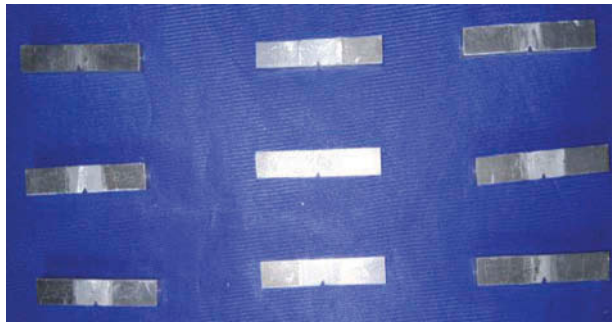

Figure 5. Specimens of impact testing.

multiple responses of problem optimize inadequate by Taguchi. The analyzing and solving of responses multiple for engineering problems. GRA of Taguchi is the best method. In 1982, Deng suggested that GRA analyses incomplete or unknown information about the outcome of different responses of parameters. Figure 6 shows the flowchart of the steps of the GRA technique.

Table 4. Different responses on average values of response

Sno	Rotational speed (rpm)	Welding speed (mm/min)	Tilt angle (degree)	Tensile strength (MPa)	Impact strength (J)	Elongation (%)
1	1,150	40	1	162.3	8.5	10.25
2	1,250	40	2	149.18	9.43	6.63
3	1,350	40	3	141.5	12	5.69
4	1,150	50	1	180.87	11.8	10.28
5	1,250	50	2	190.59	12	9.22
6	1,350	50	3	179.04	13.8	10.38
7	1,150	60	1	161.37	11	9.97
8	1,250	60	2	178.35	9	8.89
9	1,350	60	3	175.77	10.8	11.24

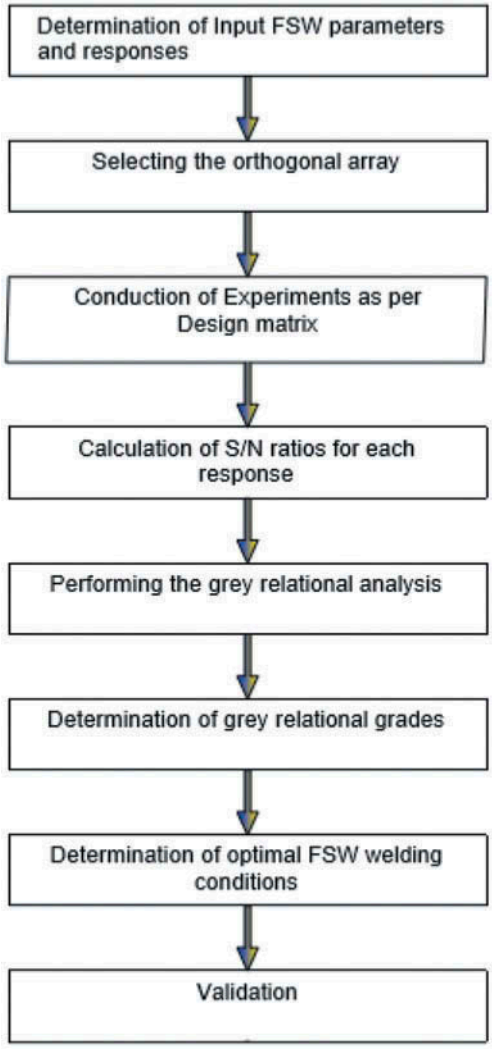

Figure 6. Flowchart of the GRA Technique.

3.1. Grey relational generation

The analysis of preprocessing data is also called a generation of Grey relation. The relational sequence of data composed values of experiments is formed in comparable sequence interval 0 and 1. Three different quality characteristics are applied: nominal is better, larger is better, and smaller is better in most parts performed. The original sequence is minimizing 'smaller the better 'characteristic used normalize sequence reference.

Selected quality characteristic type is "large is better" with the calculation of Grey relational generation Equation (1)

$$x_i^*(k) = \frac{x_i^0(k) - min\ x_i^0(k)}{\max\ x_i^0(k) - min\ x_i^0(k)} \tag{1}$$

Although $x_i^0(k)$ of series max $x_i^0(k)$ as well as min $x_i^0(k)$ is max together with min series of values,$x_i^*(k)$ after data processing generation of sequence.

i = 1,2,3....m and k = 1,2,3.... n, data of experimental is n and experiments of m.

3.2. Coefficient of Grey relation

For normalizing of process, the coefficient of Grey relational is calculated to identify the relationship between comparability sequence and the reference sequence.

Grey relational coefficients and the corresponding variations were calculated using Equations (2) and (3).

$$\Delta_{0i}(k) = \left|x_0^*(k) - x_i^0(k)\right| \tag{2}$$

$$\zeta_i(k) = \frac{\Delta_{min} + \zeta.\Delta_{max}}{\Delta_{0i}(k) + \zeta.\Delta_{max}} \tag{3}$$

where $\Delta_{0i}(k)$ series of variation and series of relation $x_i^0(k)$ series of interference $x_i^0(k)$,ζ identification coefficient, which generally 0.5 parameters are weightage equal.

Grey relational coefficients are calculated by the orthogonal array of L9 of Equation (3).

3.3. Grey relational grade

For compatibility series and reference series Grey relation grade performed for calculating, strong relationship and values are 0 and 1. The GRG has better relation for a higher value. Generally, for calculating Grey relation grade is a Grey relational coefficient average summation of Equation (4).

$$\gamma_i = \frac{1}{n}\sum_{k=1}^{n} \zeta_i(k) \tag{4}$$

Although γ_i is Grey relational grade execution of characteristics of number n experiment i^{th}. The normalized or ideal value is closer to experimental results and corresponds to GRG of larger value.

3.4. Parameter prediction for optimal value

The effects of different parameters are calculated and the best response of Grey relational grade is closer as a 1 and optimal welding condition of parameters has the highest mean GRG value.

3.5. ANOVA performance

Statistical significance of different parameters for performance of ANOVA probability p-value has used and the contribution of parameter response can resolute results of ANOVA.

Table 5. Responses of Signal-to-noise-ratios

	Raw data for responses								S/N ratios			
Experiment number	**T1**	**T2**	**T3**	**I1**	**I2**	**I3**	**E1**	**E2**	**E3**	**S/N_{TS}**	**S/N_{IS}**	**S/N_{EL}**
1	161	162	163	8.6	8.5	8.7	10	10.2	10.4	47.309	8.786	36.777
2	148	149	150	9.5	9.4	9.3	6.43	6.63	6.83	49.484	9.827	37.025
3	142	141	140	11.9	12	12.1	5.59	5.69	5.79	48.198	11.364	37.266
4	181	180	179	11.6	11.8	12	10.1	10.2	10.3	47.676	13.979	37.952
5	189	190	191	11.8	12	12.2	9.12	9.22	9.32	49.966	14.320	37.841
6	178	179	180	13.7	13.8	13.9	10.1	10.3	10.5	48.595	15.268	37.729
7	162	161	160	10.9	11	11.1	9.95	9.97	9.99	47.640	16.096	37.616
8	177	178	179	8.9	9	9.1	8.79	8.89	8.99	49.337	15.706	37.266
9	176	175	174	10.6	10.8	11	11.1	11.2	11.3	48.062	16.521	37.729

Table 6. Sequence variation and after processing data responses in series

	Reference sequence					
	Processing data after series			Reponses of series variation		
	Tensile strength	Elongation	Impact strength	Tensile strength	Elongation	Impact strength
Experiment. no	1.000	1.000	1.000	1.000	1.000	1.000
1	0.818,592	0	0	0.1,814,076	1	1
2	0.334,588	0.1,345,831	0.2,110,638	0.6,654,121	0.8,654,169	0.7,889,362
3	0.138,126	0.3,332,902	0.4,161,702	0.8,618,743	0.6,667,098	0.5,838,298
4	1	0.6,713,639	1	1.33,115	0.3,286,361	2.442,115
5	0.484,005	0.7,154,493	0.9,055,319	0.5,159,955	0.2,845,507	0.0944681
6	0.124,577	0.838,009	0.8,102,128	0.8,754,234	0.161,991	0.1,897,872
7	0.763,267	0.9,450,549	0.7,140,426	0.2,367,332	0.0549451	0.2,859,574
8	0.283,402	0.8,946,348	0.4,161,702	0.7,165,977	0.1,053,652	0.5,838,298
9	0	1	0.8,102,128	1	2.22,116	0.1,897,872

Table 7. GRGs and GRCs of estimation

	Coefficient of Grey relation			GRG	Rank
Experiment. number	**Tensile strength**	**Elongation**	**Impact strength**		
1	0.7,337,752	0.3,333,333	0.3,333,333	0.1,778,514	7
2	0.4,290,328	0.3,661,885	0.3,879,168	0.1,339,854	9
3	0.3,671,411	0.4,285,556	0.4,613,271	0.1,348,009	8
4	1	0.6,034,012	1	0.2,936,735	1
5	0.4,921,282	0.6,373,074	0.841,088	0.2,018,246	4
6	0.3,635,244	0.7,552,973	0.7,248,612	0.1,844,412	5
7	0.6,786,718	0.9,009,901	0.6,361,668	0.2,456,221	2
8	0.4,109,822	0.8,259,477	0.4,613,271	0.1,818,469	6
9	0.3,333,333	1	0.7,248,612	0.2,038,796	3

3.6. Prediction parameters for optimal level

The optimal level of different parameters for resolution of prediction of GRG value by using Equation (5)

$$\gamma_e = \gamma_m + \sum_{i=1}^{q}(\overline{\gamma_i} - \gamma_m) \tag{5}$$

Although γ_m is mean total of GRG, q is parameter number, $\overline{\gamma_i}$ is GRG mean value of optimal level qth parameter.

3.7. Signal-to-noise ratio

Table 4 represents responses of average values of input parameter settings. The responses of the three parameters are calculated by the signal-to-noise ratio. Higher values of tensile strength, elongation, and impact strength give better performance of welding. Equation (6) is a signal-to-noise ratio for calculation. The mechanical testing is executed on three responses. The testing results of the FSW joint of ratios S/N are shown in Table 5.

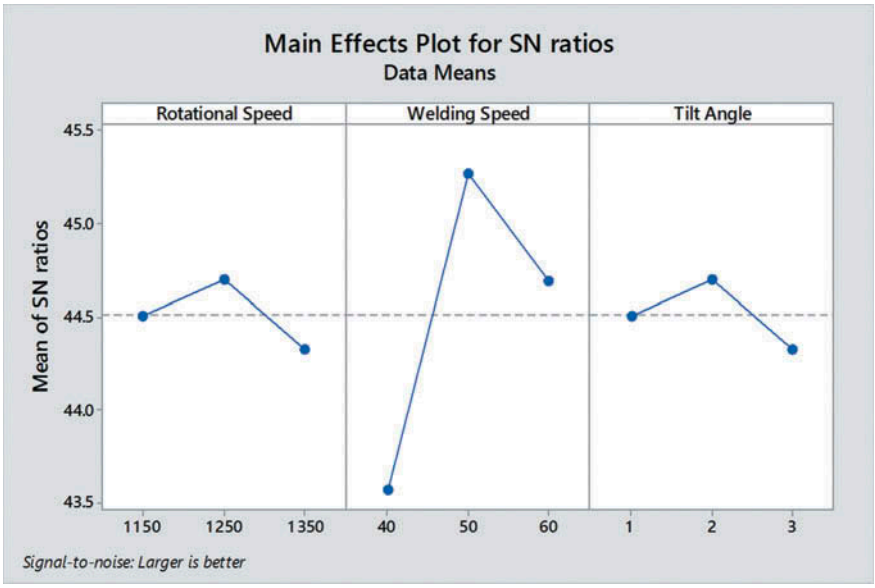

Figure 7. Main effects plot of tensile strength for signal-to-noise-ratio.

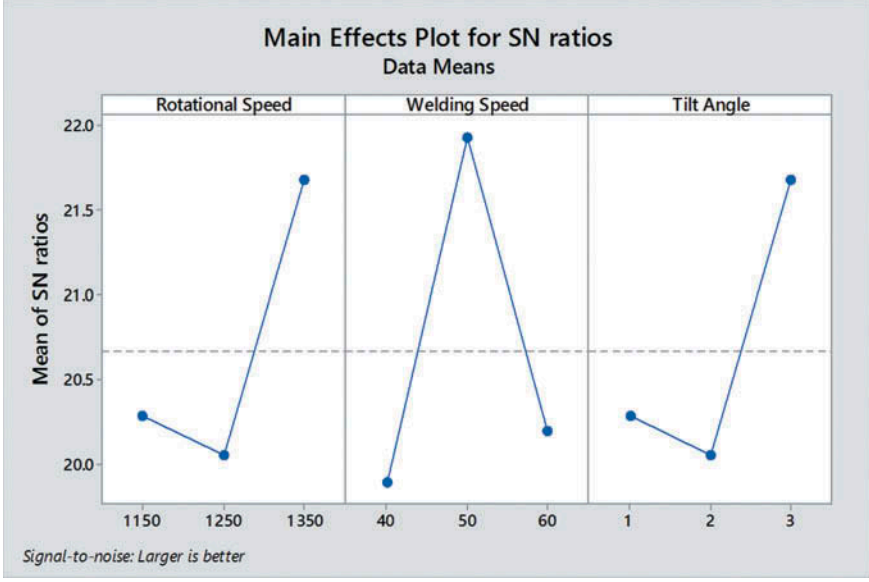

Figure 8. Main effects plot of impact strength for signal-to-noise-ratio.

$$\text{Signal}-\text{to}-\text{noise ratio} = -10log_{10}\left(\frac{1}{n}\right)\sum_{i=1}^{n}\frac{1}{y^2_{ijk}} \quad (6)$$

Although experimental reproduction of n number and Y_{ijk} variable response of *i*th characteristic execution of experiment *j*th experiment with trail *k*th.

3.8. Sequence deviation and data processing calculation

The analysis part for S/N ratio normalize value for response Equation (1) and S/N ratios are given in Table 5. For calculations of the coefficient of Grey relation, sequence deviation is determined. The calculations are shown in Table 6.

Figure 9. Main effects plot of elongation for signal-to-noise-ratio.

3.9. Grey relational coefficients and grade estimation

The estimation of GRCs by Equation (3) sequence deviation shown in Table 6. The ζ characteristic are designate value as 0.5 and performances of trademark and Equation (3) is calculated by grey relation coefficients for estimated values GRCs and GRGs shown in Table 7.

The GRC values of nine experiments are calculated by Equation (1). The characteristic performance of GRGs is determined in Equation (4). The values of weight tensile strength, elongation, and impact strength are 0.5, 0.3, and 0.2.

3.10. Input parameters of optimum levels estimation

The parameters of each level for the calculation of signal-to-noise-ratio value is considered: rotational speed RS 1,250 rpm, welding speed WS 50 mm/min, and tilt angle TA 2°are better characteristics performance of S/N ratios shown in Figure 7.

The parameters on each level for signal-to-noise-ratio calculation value is considered rotational speed RS 1350 rpm, welding speed WS 50 mm/min and tilt angle TA 3°are better characteristics performance of S/N ratios shown in Figure 8.

The parameters on each level for signal-to-noise-ratio calculation value is considered rotational speed RS 1350 rpm, welding speed WS 50 mm/min and tilt angle TA 3°are better characteristics performance of S/N ratios shown in Figure 9.

4. Microstructural investigations

Figure 10 shows the microstructural investigations on different zones and Figure 10(a) shows the microstructures with magnification 100× and Etchant is HydroFluoric solution. AA 6082 in cold rolled condition with grain orientation along the direction of rolling with eutectic and insoluble constituents. Figure 10(b) shows the shoulder zone of the FSW process and the metal matrix underwent fragmentation due to the stirring and the frictional heat of the process facilitated the dissolution of the eutectic constituents of both 7075 and 6082. Alternate layers of 6082 and 7075 constituents underwent fragmentation and recrystallization. Figure 10(c) shows the heat-affected zone of AA 6082 close to the nugget zone with grain orientation with the formation of TMT ring at the top and bottom of the zone. Figure 10(d) shows the interface zone of the AA6082 and the nugget zone at the bottom of the FSW zone. Figure 10(e) shows the bottom of the nugget zone center with a substantial flow of 6,082

Figure 10. Microstructural investigations on different zones.

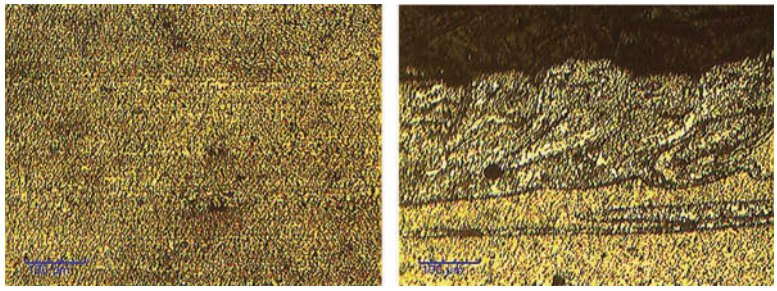

(a) AA 6082 in cold rolled condition

(b) Eutectic constituents of both 7075 and 6082

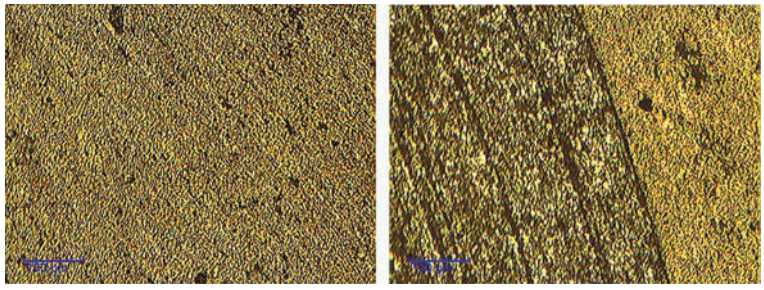

(c) Heat affected zone of AA 6082

(d) Interface zone of the AA6082

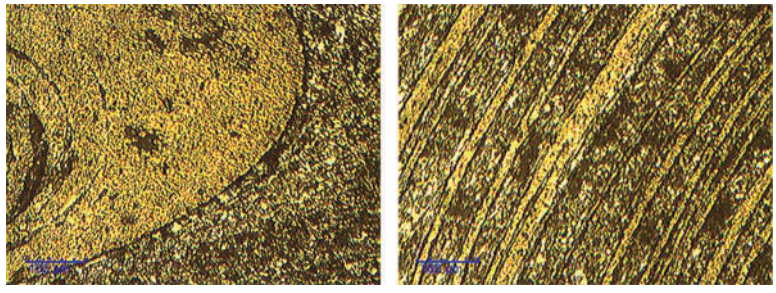

(e) Nugget zone center

(f) Nugget zone bottom where 7075 & 6082

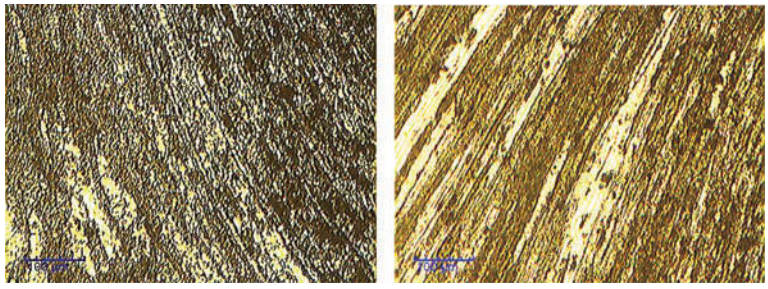

(g) Interface zone of the nugget of AA 7075

(h) TMT zone of the AA 7075

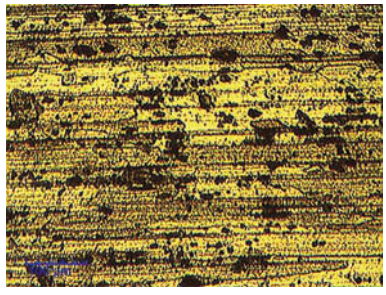

(i) AA 7075 parent metal at the advancing side

constituents. Figure 10(f) shows the nugget zone bottom where 7075 and 6082 have undergone effective and enhanced plasticity, leading to the formation of alternate layers with equal intervals. Figure 10(g) shows the interface zone of the nugget and the AA 7075 at left side and nugget at the right side. The grain orientation of the 7075 towards downwards observed at the interface. Figure 10 (h) shows the thermomechanical transformation zone of the AA 7075 where the heat of the process increases the plasticity of the parent metal and metal has undergone plastic deformation in the direction of the tool. The flow of grains shows higher plasticity caused due to a higher temperature at this zone due to mechanical parameters. The eutectic constituents have also undergone deformation. Figure 10(i) shows the microstructure of AA 7075 parent metal at the advancing side of the FSW process. The parent metal shows microstructure in rolled temper condition. The sheet has been cold worked by the rolling process, and the primary grains of alpha aluminum are elongated along with the direction of formation. The eutectic constituents such as Cu-Al_2, Mg_2Si, Zn-Al_2, and Mg-Al_2 precipitated along the rolling direction and elongated.

5. Conclusions

(1) The multi-responses, i.e. tensile strength 190 MPa, impact strength 12J, and elongation 9.22 %, were optimized using Grey–Taguchi-based relational analysis method.

(2) The research was carried out by varying rotational speed 1,250 rpm, weld speed 50 mm/min, and tilt angle 2°.

(3) After carrying out experiments as per the experimental plan, outputs were measured and tabulated.

(4) This experimental data was used for further analysis using the GRA method. In this method, signal-to-noise ratios and grey relational coefficients, and grey relational grades 0.2893 and rank 1 at maximum grade at welding condition.

(5) The individual graphs present the exact trend between inputs and outputs.

(6) This method is a very successful optimizing technique for improvement of microstructures on the nugget zone and thermomechanical transformation zone.

Acknowledgments
With a profound feeling of appreciation, we recognize the direction, help, and dynamic participation rendered by the accompanying individuals whose direction has supported the exertion which prompted effective finish. The authors would like to express deep gratitude to Prof V. Balasubramanian from Annamalai University, for providing equipment facilities. In conclusion, we express for the support entire research of my supervisior Dr. G. Harinath Gowd, Professor, Madanapalle Institute of Technology and Science, Prof. B. Durga Prasad, professor, JNTUACE, Ananthapauramu because of each one of the individuals who has been useful straightforwardly in bringing the paper.

Funding
The authors received no direct funding for this research.

Author details
Bazani Shaik[1]
E-mail: bazanimits@gmail.com
ORCID ID: http://orcid.org/0000-0001-8155-2533
G. Harinath Gowd[2]
E-mail: gowdmits@gmail.com
B. Durga Prasad[3]
E-mail: mukdhajntu@gmail.com
[1] Department of Mechanical Engineering, JNTUA, Ananthapuramu, India.
[2] Department of Mechanical Engineering, Madanapalle Institute of Technology and Science, Madanapalle, India.
[3] Department of Mechanical Engineering, JNTUA College of Engineering, Ananthapuramu, India.

Citation information
Cite this article as: Investigations and optimization of friction stir welding process to improve microstructures of aluminum alloys, Bazani Shaik, G. Harinath Gowd & B. Durga Prasad, *Cogent Engineering* (2019), 6: 1616373.

References

Dourandish, S., Mousavizade, S. M., Ezatpour, H. R., & Ebrahimi, G. R. (2017). Microstructure, mechanical properties and failure behavior of protrusion friction stir spot welded 2024 aluminum alloy sheets. *Science and Technology of Welding and Joining*. doi:10.1080/13621718.2017.1386759

Giraud, L., Robe, H., Claudin, C., ChristopheDesrayaud, P., & Bocher, E. F. (2016). Investigation into the dissimilarfrictionstirweldingofAA7020T651andA-A6060T6. *Journal of Materials Processing Technology*. doi:10.16/j.jmatprotec.2016.04.020

Han, W., Wan, F., Yabuuchi, K., Serizawa, H., & Kimura, A. (2018). Joint inhomogeneity in dissimilar friction stir welded martensitic and nanostructured ferritic steels. *Science and Technology of Welding and Joining*. doi:10.1080/13621718.2018.1456797

IzabelaKalemba-Rec, K. (2018, May). Effect of process parameters on mechanical properties of friction stir welded dissimilar 7075-T651 and 5083-H111 aluminum alloys. *International Journal of Advanced Manufacturing Technology*. doi:10.1007/s00170-018-2147-y

Kaiser, M. S. (2018, January June). Solution Treatment Effect on Tensile, Impact and Fracture Behavior of Trace Zr Added Al–12Si–1Mg–1Cu Piston Alloy. *Journal of the Institution of Engineers (India):*

Series D, *99*(1), 109–114. doi:10.1007/s40033-017-0140-5

Khan, N., Siddiquee, A. N., Khan, Z. A., et.al (2018). Microstructure evolution of friction stir welded dissimilar aerospace aluminium alloys. *IOP Conference Series: Materials Science and Engineering*, *404*, 012002. doi:10.1088/1757-899X/404/1/012002

Li, P., Yu, G., Wen, H., Guo, W., & Tong, X. (2018). Li Friction stir welding between the high-pressure die casting of AZ91 magnesium alloy and A383 aluminum alloy. *Journal of Materials Processing Tech*. doi:10.1016/j.jmatprotec.2018.08.044

Liu, G. L., Yang, S. W., Han, W. T., Zhou, L. J., Zhang, M. Q., Ding, J. W., … Misra, R. D. K. (2018a). Microstructural evolution of dissimilar welded joints between reduced-activation ferritic-martensitic steel and 316L stainless steel during the post weld heat treatment. *Materials Science & Engineering A*. doi:10.1016/j.msea.2018.03.035

Liu, Z., Yue, Y., Zhang, W., et.al. 2018b. Interface behavior, and lap shear properties of the 7075-T6 Al FSLW joint using a tip-threaded pin. *TransIndianInst Metals*. doi:10.1007/s12666-018-1360-6,

Padhy, G. K., Wu, C. S., & Gao, S. (2018). Friction stir based welding and processing technologies - processes, parameters, microstructure, and applications: A review. *Journal of Materials Science & Technology*, *34*, 1–38. doi:10.1016/j.jmst.2017.11.029

Rajesh, G., Srimuthunath, I., Santa Kumar, N., Sugandipriya, S., & Aravindan, V. (2018). Characterization of microstructure and hardness of friction stir welded brass plate. *Materials Today: Proceedings*, *5*, 2721–2725.

SachinKumar, Rabindranath, S., et.al (2018). *Process parameter optimization for FSW of AA6061/Sic/Fly Ash iMacs using Taguchi Technique*. ICE Publishing.

Santos, T. F. D. A., Torres, E. A., & Ramirez, A. J. (2017). Friction stir welding of duplex stainless steels. *Welding International*. doi:10.1080/09507116.2017.1347323

Sundqvist, J., Kim, K.-H., Bang, H.-S., Bang, H.-S., Alexander, F. H., & Kaplan. (2017). Numerical simulation of laser preheating of friction stir welding of dissimilar metals. *Science and Technology of Welding and Joining*. doi:10.1080/13621718.2017.1391936

Wahid, M. A., Khan, Z. A., Siddique, A. N., Shandley, R., & Sharma, N. (2018). Analysis of process parameters effects on underwater friction stir welding of aluminum alloy 6082-T6. *Journal of Engineering Manufacture-Institution of Mechanical Engineers*. doi:10.1177/0954405418789982

Wahid, M. A., Siddique, A. N., Khan, Z. A., et.al. 2018. Friction stir welding of AA-5754 in water and air: A comparative study. *Materials Research Express in Press*. doi:10.1088/20531591/aae6fd